Pharm Res (2015) 32:3282–3292
DOI 10.1007/s11095-015-1706-2

RESEARCH PAPER

Phytantriol Based "Stealth" Lyotropic Liquid Crystalline Nanoparticles for Improved Antitumor Efficacy and Reduced Toxicity of Docetaxel

Sanyog Jain[1] • Neha Bhankur[1] • Nitin K. Swarnakar[1] • Kaushik Thanki[1]

Received: 4 March 2015 / Accepted: 4 May 2015 / Published online: 13 May 2015

ABSTRACT

Purpose The present work focuses on design and development of surface functionalized LCNPs for improving tumor delivery of DTX.

Methods Phytantriol based "stealth" LCNPs were prepared using hydrotrope method and optimized. The potential of developed formulation was further assessed using cell culture experiments, *in vivo* pharmacokinetics, *in vivo* pharmacodynamics and toxicity studies.

Results A biphasic drug release pattern was observed with sustained release of drug till 72 h. *In vitro* cell culture experiments revealed efficient internalization within MCF-7 cells with 25.80-fold decrease in IC_{50} value for PEG-LCNPs as compared to free DTX. Mechanistic insights demonstrated preferential co-localization of LCNPs in the vicinity of the nucleus. Furthermore, *in vivo* pharmacokinetic studies revealed 14.45-fold enhancement in circulation half-life of PEG-LCNPs as compared to marketed formulation Taxotere®. *In vivo* efficacy studies PEG-LCNPs in DMBA induced breast cancer model revealed ~81% reduction in the tumor burden compared to Taxotere® which caused/achieve only 47% reduction or showed only 47% decrease. Furthermore, safety profile was noted for PEG-LCNPs as compared to Taxotere®, measured as a function of hepato- and nephro-toxicity.

Conclusions Surface functionalization of LCNPsis a viable approach for improving the therapeutic potential of DTX.

KEY WORDS DMDA model · docetaxel · *in vivo* antitumor efficacy · liquid crystalline nanoparticles (LCNPs) · PEGylation · surface functionalization

ABBREVIATIONS

ALT	Alanine aminotransferase
AST	Aspartate aminotransferase
AUC	Area under curve
BUN	Blood urea nitrogen
CLSM	Confocal laser scanning microscope
CoQ10	Coenzyme Q 10
DAPI	4′,6-diamidino-2-phenylindole
DMBA	7,12-dimethylbenz[a]anthracene
DSPE	1, 2-Distearoyl-sn-glycero-3-phospho-ethanolamine
DTX	Docetaxel
EPR	Enhanced permeation and retention
FBS	Fetal bovine serum
FDA	Food and Drugs Administration
GMO	Glyceryl monooleate
HBSS	Hanks's balanced salt solution
IAEC	Institutional animal ethics committee
ICH	International conference on harmonization
LCNPs	Liquid crystalline nanoparticles
MCF-7	Human adenocarcinoma breast cancer cell line
MRT	Mean residence time
MTT	(3-(4,5-Dimethyl-2-thiazolyl)-2,5-diphenyl-2H-tetrazolium bromide)
PDI	Polydispersity index
PEG	Polyethylene glycol
SAXS	Small angle X ray spectroscopy
TEM	Transmission electron microscopy

This work is a part of Indian Patent Application No. 680/DEL/2013 filed on March 08 2013

Electronic supplementary material The online version of this article (doi:10.1007/s11095-015-1706-2) contains supplementary material, which is available to authorized users.

✉ Sanyog Jain
sanyogjain@niper.ac.in; sanyogjain@rediffmail.com

[1] Centre for Pharmaceutical Nanotechnology, Department of Pharmaceutics, National Institute of Pharmaceutical Education and Research (NIPER), Sector 67, S.A.S., Nagar (Mohali), Punjab 160062, India

INTRODUCTION

Docetaxel (DTX) is a potent second generation taxane with broad antineoplastic action against series of cancer types such as non-small cell lung cancer, prostate, breast, gastric cancer, etc. (1). Taxotere®, containing docetaxel with polysorbate 80 and ethanol was first approved by FDA in 1996 for anthracycline-resistant metastatic breast cancer (2). This formulation contains polysorbate 80 and ethanol to solubilize the lipophilic drug, DTX. However, the excipients of the formulation show deleterious effects in body. Polysorbate 80 increases the free drug levels in the blood by affecting the protein binding of DTX which leads to hematological toxicity (3). In addition, anaphylactic reactions (e.g., hypersensitivity, fluid retention) have also been reported in patients which could not be prevented completely even after pre-medication with corticosteroids (4). Hence, development of safe and efficacious delivery strategy for DTX remains a challenging task for scientists, until today. In purview of this, many alternative formulations of DTX such as liposomes, polymeric nanoparticles, micelles and solid lipid nanoparticles have been investigated. Among the various available nanocarriers, liquid crystalline nanoparticles (LCNPs) can be a multifaceted innovative carrier for cancer therapy (5–7).

Self-assembled liquid crystalline nanoparticles were first reported by Luzzati *et al.* which revealed their bicontinuous cubic structures (8). They represent a novel class of nanocarriers, which have drawn substantial attention with regards to drug delivery due to their unique properties such as sustained release, biocompatibility, solubilization and unique ability to entrap hydrophilic, lipophilic as well as amphiphilic drugs (6, 9, 10). The constituents of LCNPs show different self-assembly structures/phases like alkanols form solid solutions, fatty acids form only liquids and fatty amines being capable of forming a binary liquid crystalline phase. The latter are also formed by glycerides/lipids/ fatty acids containing two OH groups such as monoglycerides, hexadecane-1,2-diol and α-hydroxypalmitic acid (11). However, there exists limited number of polar lipids eg which are capable of forming LCNPs. Conventionally, glyceryl mono/di oleate, phytantriol, glycerates, glycolipids, etc. have been available (12). Among these, glyceryl mono oleate (GMO) has been classically employed for the formation of LCNPs and improving the deliverability of therapeutics. However, GMO exhibits haemolytic toxicity which limit its use in intravenous formulations (13). Recently, phytantriol has emerged as a safer lipid excipient for development of LCNPs (14). Our group has exhaustively explored phytantriol based LCNPs for improving the oral delivery of doxorubicin and Coenzyme Q10 considering its unique properties of indigestibility against gastrointestinal lipases and serum esterases (7, 15).

The therapeutic efficacy and biodistribution profile of nanoparticles have been extensively tailored using/by surface functionalization (16, 17). Among various available surface modification molecules/ functional groups, PEGylation approach is the most classical and is regarded as the most simple yet highly effective technique for surface modification (18). PEGylated liposomes of doxorubicin (Doxil®) have already paved its way on/to or onto the clinical bedside suggesting relatively higher industrial scalability and adaptability of PEGylated systems (19). Recent advances in the field of PEGylation have enabled availability of functionally terminated PEGs thereby simplifying the conjugation approaches and ensuring rapid product development.

The present work focuses on the design and development of surface functionalized LCNPs comprising of phytantriol as lipidic excipient and 1, 2-Distearoyl-sn-glycero-3-phosphoethanolamine (DSPE) linked PEG as surface modifier for improving the tumor delivery of DTX.

MATERIALS AND METHODS

Materials

Docetaxel (DTX) and Phytantriol (3,7,11,15-tetramethyl-1,2,3-hexadecanetriol) were obtained as generous gift from Fresenius Kabi Oncology, India and DSM Nutritional Products, Inc., Germany, respectively. Various grades of Pluronic® (F-108, F-127, F-68 and F-87) were procured from BASF, Germany as gift sample. N-(Carbonyl-methoxypolyethylenglycol-2000)-1, 2-distearoyl-sn-glycero-3-phosphoethanolamine, MPEG-2000-DSPE, Na-salt was obtained as a gift sample from Lipoid, Germany. 7,12-dimethylbenz[a]anthracene (DMBA), Trypsin-EDTA, MTT (3-(4,5-Dimethyl-2-thiazolyl)-2,5-diphenyl-2H-tetrazolium bromide), coumarin-6, triton X-100, mannitol, fetal bovine serum (FBS), antibiotics (Antibiotic-antimycotic solution), Hanks's balanced salt solution (HBSS) and 4′,6-diamidino-2-phenylindole (DAPI) were procured from Sigma Aldrich, USA. Cell culture plates (6-well and 96-well) were procured from Becton Dickinson, USA. Acetone (AR grade), acetonitrile (HPLC grade) and methanol (HPLC grade) were purchased from Merck, India. Ultra-pure deionized water (LaboStar™ ultrapure water Systems, Germany) was used for all the experiments. All other reagents used were of analytical grade and purchased from local suppliers unless mentioned.

Preparation, Optimization and Lyophilization of DTX Loaded LCNPs

Two different types of DTX loaded LCNPs i.e., LCNPs-DTX and PEG-LCNPs-DTX were prepared by hydrotrope method (15). Briefly, DTX and phytantriol were dissolved in ethanol (2.5%*v*/*v* with respect to dispersion). The obtained isotropic solution was then added drop-wise to aqueous surfactant solution (0.5%*w*/*v* Pluronic F108). The resulting dispersion was then stirred at 2000 rpm for 12 h to evaporate ethanol

leading to the formation of DTX-LCNPs. In a separate set of experiments, the surface functionalized lipids for anchoring purposes, N-(Carbonyl-methoxy-polyethylenglycol-2000)-1, 2-distearoyl-sn-glycero-3-phospho-ethanola-mine, MPEG-2000-DSPE, Na-salt was employed. The surface functionalized LCNPs were prepared in similar manner by additionally supplementing the hydroptope solution with PEG-DSPE Subsequently, exhaustive optimization of the variables was carried out as described in Table S1 (Supplementary information). Optimized formulations were then freeze dried by/according to using mannitol (5%*w*/*v*) as cryo-protectant (15).

Characterization of DTX Loaded LCNPs

The optimized formulations of DTX loaded LCNPs were evaluated for particle size, poly-dispersity index (PDI), zeta potential and entrapment efficiency following standard protocols (20). The shape and surface morphology was characterized using transmission electron microscopy (TEM) and small angle X-ray scattering analysis (SAXS) following standard procedures (15, 21). The developed formulations were also subjected to accelerated stability studies as per International Conference on Harmonization (ICH) guidelines (20).

In Vitro Drug Release

The *in vitro* release of DTX from various LCNPs was carried out by dialysis membrane method. Briefly, phosphate buffer (pH 7.4 and 5.5) with and without 10%*v*/*v* fetal bovine serum (US origin, Sigma USA) supplemented with 0.1% Tween 80 were employed as release media. Lyophilized formulations equivalent to 2 mg DTX were reconstituted and filled in the dialysis bag (Mol wt cutoff, 12KD, Sigma USA). The whole setup was then suspended in the release media and aliquots of 200 µl were withdrawn at predetermined time intervals and analysed by validated HPLC method. The equivalent amount of fresh media was replenished after every time interval. Cumulative release (%) was plotted as a function of time and curve fitted (21).

Cell Culture Experiments

MCF-7 (Human adenocarcinoma breast cancer cell line) was maintained as per standard procedures reported earlier by our group (22). Cell viability studies of various developed formulations against MCF-7 cell line were evaluated. Briefly, MCF-7 cells in confluent stage were harvested and seeded into 96 well plates (Costars, Corning Inc.) at a cell density of 10^4 cells/well. The cells were then incubated with different concentrations (0.1, 0.5, 1 and 10 µg/ml) of DTX loaded LCNPs for 24, 48 and 72 h. Upon completion of the incubation period, cells were processed for MTT assay as per standard protocol (23). Further the mechanistic insights on cell cytotoxicity potential was also assessed using nuclear localization studies and apoptotic assay. Briefly, cells were seeded in 6-well plate at cell density of 1,00,000 cells/well and allowed to adhere overnight. For nuclear co-localization studies, coumarin-6 co-loaded DTX LCNPs equivalent to 5 µg/ml of DTX were exposed to the cells for stipulated period of time. Subsequently, the cells were washed and counterstained with DAPI to tag nucleus and visualised for intracellular trafficking of the developed formulations. For apoptosis assay also, seeded cells were incubated with various DTX loaded LCNPs and subsequently cells were processed for apoptosis assay as per manufacturer's protocol (Annexin V-Cy3™ Apoptosis Detection Kit, Sigma, USA). The kit comprised of double stains: 6-Carboxyfluorescein diacetate detecting live cells and Annexin V-Cy3.18 conjugate detecting apoptotic cells. The cells were then washed and observed under confocal laser scanning microscope (CLSM, Olympus, Japan). Apoptosis index, ratio of the fluorescence intensity from the red channel (originated from the Annexin V conjugate) to that of green channel (originated from 6-Carboxyfluorescein diacetate) was calculated. The quantitative measure of fluorescence within the images was processed with CLSM software (FluoView 4.0, Olympus).

In Vivo Pharmacokinetics

In vivo pharmacokinetic studies were performed in female Sprague Dawley rats (220–250 g). All the animal study protocols were duly approved by Institutional Animal Ethics Committee (IAEC), NIPER, India. Animals were housed in standard housing conditions and randomly divided in to four groups each containing six animals. Groups 1–4 received DTX solution (in PEG 400), Taxotere®, LCNPs-DTX and PEG-LCNPs-DTX, respectively. The formulations were injected by intravenous route in SD rats by tail vein at a dose of 2 mg/kg body weight of the animal.(24) The blood samples (~0.5 ml) were collected from the retro orbital plexus of eye under mild anesthesia into heparinized micro centrifuge tubes (containing 30 µl of 1000 U of heparin). The collected blood samples were processed for separation of plasma by centrifuging at 5000 g for 5 min at 15°C. About 25 µl of internal standard (1-amino 4-nitro naphthalene) was added to 250 µl plasma and then vortexed for 1 min. Subsequently, 500 µl of acetonitrile was added to the plasma samples for precipitating the proteins and extracting the drug. The samples were vortexed further for 15 min. The resulting mixture was then centrifuged at 15,000 g for 5 min and supernatant was dried at 40°C in vacuum oven. The dried samples were then redispersed in 90 µl acetonitrile, vortexed and centrifuged at 15,000 g for 5 min. The supernatants were analyzed for drug content by validated HPLC method (Supplementary information). The obtained plasma concentration time profile was analyzed by biphasic clearance kinetics using Kinetica Software (Version 5.0, Thermo scientific) and estimated for

total area under the curve $(AUC)_{0-\infty}$, terminal phase half-life ($t_{1/2}$), mean residence time (MRT) and clearance (CL).

In Vivo Antitumor Efficacy

Experimental tumors in female Sprague Dawley (SD) rats (weighing 220–250 g) were chemically induced by 7, 12-dimethylbenzanthracene (DMBA) Briefly, DMBA was solubilized in soya bean oil and administered orally to rats at a dose of 45 mg/kg after every week for three consecutive weeks (20, 25). It has been classically known that DMBA induces palpable multiple tumors preferably within breast region. However, owing to the anticipated lymphatic absorption of DMBA from gastrointestinal tract, at times tumors also emerge at lymph nodes across the body. In purview of this, desired tumor or set of tumors are marked which would be subsequently monitored while assessing the efficacy of the formulation treatment. The tumor bearing animals were segregated randomly into three treatment groups each for single dose of DTX-LCNPs (i.v.), DTX-PEG-LCNPs (i.v.), and Taxotere® (i.v.) equivalent to 2 mg DTX /kg of body weight. Each group comprised of 6 animals. The tumor size was monitored up to 10 days after the administration of formulation and the tumor width and length were recorded using vernier caliper. In a separate set of experiments, coumarin-6 co-loaded DTX formulations were injected intravenously to the fresh tumor induced animals *via* tail vein. After 2 h, the animals were sacrificed and tumor tissues were excised, washed with phosphate buffer saline and fluorescence of coumarin-6 was visualized using Live Non-invasive Animal Photon Imager (Biospace, France) (7).

Toxicity Studies

The safety profile of the developed formulations was established by carrying out toxicity studies in healthy female Swiss albino mice (~25 g). Briefly, mice were randomly divided into four groups (5 mice per group) – control, LCNPs-DTX, PEG-LCNPs-DTX, and Taxotere® (prophylactic treatment with corticosteroids). All the formulations were administered intravenously at the equivalent DTX dose of 2 mg/kg. After 7 days of treatment, blood samples were collected in heparinized micro-centrifuge tubes and centrifuged at 5000 g for 5 min to separate plasma. Various biochemical parameters such as creatinine levels, urea and blood urea nitrogen (BUN) levels for nephrotoxicity; alanine aminotransferase (ALT) and aspartate aminotransferase (AST) were monitored as hepatotoxicity markers (21). The biochemical parameters were determined spectrophotometrically according to the manufacturers guidelines for the diagnostic kits obtained from Accurex (Accurex biomedical Pvt. Ltd., India).

Statistical Analysis

All the data are expressed as mean ± standard deviation (SD) for all *in-vitro* and mean ± standard error of mean (SEM) for all *in-vivo* results. Statistical analysis was performed using SigmaStat (version 3.5) utilizing one-way ANOVA followed by Tukey-Kramer multiple comparison test. $p<0.05$ was considered as statistically significant difference.

RESULTS

Preparation and Evaluation of DTX Loaded LCNPs

Hydrotrope method was employed for preparation of DTX loaded LCNPs. All the batches of LCNPs dispersions were subjected to polarized light microscopy based in-process quality control which revealed dark diffraction pattern suggestive of isotropic behaviour. By virtue of exhaustive optimization of the formulation components and process variables a set of parameters were found to have LCNPs with particle size <200 nm, entrapment efficiency >80%, and acceptable PDI at 5% theoretical drug loading (Table S2-S6). The optimized formulations were then lyophilized using 5%*w*/*v* mannitol as cryo-protectant (Supplementary information, S3). Table I depicts the quality attributes of optimized formulations prepared at 5% theoretical drug loading, using Pluronic F 108 (0.5%*w*/*v*) as surfactant and ethanol (2.5%*v*/*v*) as hydrotrope.

Figure 1 and Table II represents TEM images and SAXS diffraction pattern of blank and various DTX loaded LCNPs. Ordered texture with near-cubic structures were seen in case of blank LCNPs, while mixed cubic and hexagonal structures were seen for DTX loaded LCNPs. Furthermore, the prepared formulations were also subjected to accelerated stability studies as per ICH guidelines. Insignificant changes ($p>0.05$) were observed in physical appearance, particle size, zeta potential and % encapsulation efficiency upon subjecting all the

Table I Physiochemical Characterization of Various Formulations

Formulations	Size (nm)	PDI	Zeta Potential (mV)	Entrapment efficiency (%)	Practical loading (%)
LCNPs-DTX	161.3 ± 4.38	0.232 ± 0.03	−23.5 ± 0.78	85.52 ± 0.88	4.26%
PEG-LCNPs-DTX	193.2 ± 3.82	0.274 ± 0.08	−28.9 ± 0.63	80.40 ± 3.11	4.02%

Values are expressed in mean ± SD ($n=6$)

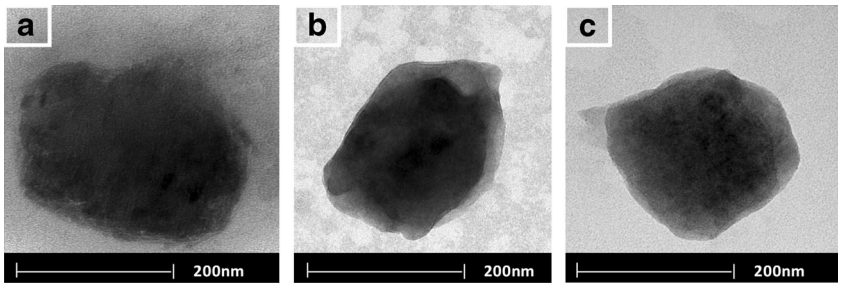

Fig. 1 TEM images of (**a**) Blank LCNPs, (**b**) LCNPs-DTX, and (**c**) PEG-LCNPs-DTX.

optimized formulations for stability studies for 6 months (Table S8, Supplementary information). Furthermore, the integrity of cake was monitored throughout stability studies and was found to be intact (Supplementary information, S3).

In Vitro Drug Release

Significant release retardation of DTX was observed from all the developed formulations as compared to free DTX (Fig. 2). Complete drug release was observed from dialysis bag within 6 h in case of DTX solution. In contrast, a biphasic drug release pattern was observed in case of developed formulations with relative rapid release in initial 24 h followed by sustained release in next 72 h (>75%). However, the extent of retardation was significantly higher ($P<0.001$) in case of PEG-LCNPs-DTX as compared to that of LCNPs-DTX. Furthermore, the release patterns were not affected in presence or absence of serum suggestive of robustness of the developed formulations. The obtained drug release pattern was then subjected to curve fitting which revealed preferential kinetics as Hixon-Crowell in case of LCNPs-DTX and Higuchi in case of PEG-LCNPs-DTX (Table III).

Cell Culture Experiments

Table IV reveal the comparative cell cytotoxicity of various DTX loaded formulations against MCF-7 cell lines. Concentration and time dependent increase in the cell cytotoxicity was observed for all the formulations (Fig. 3a). However, the magnitude of cell cytotoxicity was significantly higher in case of LCNPs formulations with IC_{50} values being ~0.228 and ~0.098 μg/ml for LCNPs-DTX and PEG-LCNPs-DTX, respectively, in contrast to ~2.529 μg/ml for free DTX when incubated for 48 h., the cell viability in case of blank formulation was >90% in case of both LCNPs and PEG-LCNPs. Apoptosis assay further revealed remarkably higher apoptotic potential of DTX loaded formulations as compared to the free drug. Among the developed formulations, PEG-LCNPs (Apoptosis index, AI,1.175) exhibited higher apoptotic potential as compared to plain LCNPs (AI 0.726) (Fig. 3b). Intracellular trafficking studies were further carried out which revealed nucleus as the preferential site for localization of developed LCNPs within the cells. The green fluorescence images in Fig. 4a and b depicts the coumarin 6 loaded LCNPs whereas the blue colour depicts the DAPI staining of the nucleus. Although both plain LCNPs and PEG-LCNPs tend to localize near nucleus, relatively higher florescence was noted in case of PEG-LCNPs. In addition, line plot analysis and box-plot analysis were further performed which further corroborated the results of co-localization studies. Quantitatively, the observed co-localization was in the range of 80–85% for both the cases (Fig. 4a, g and n).

In Vivo Pharmacokinetics

Significant difference in the pharmacokinetic profiles of various DTX formulations was observed (Fig. 5). Table V reveals various pharmacokinetic parameters of DTX loaded formulations. Although, C_{30min} was significantly higher in case of free DTX and Taxotere® as compared to that of DTX loaded LCNPs, the latter had remarkably higher half-life of the order of >12 h which in the former case was only <2 h. Among the developed formulations, PEG-LCNPs-DTX exhibited highest circulation half-life (~22 h) followed by

Table II SAXS Diffraction Pattern of Blank and Various DTX Loaded LCNPs

Formulation	Relative ratio of Bragg peaks positions	Miller indices	Structure of LCNPs	Lattice constant (Å)
Blanks LCNPs	√2: √3: √4: √5	(1,1,0) (1, 1, 1) (2,0,0) (2,1,0)	Pn3m	6.95
LCNPs-DTX	1: √3:2	(1,0,0) (1, 1, 1) (2,0,0)	H_{II}	6.51
PEG-LCNPs-DTX	1: √3:2	(1,0,0) (1, 1, 1) (2,0,0)	H_{II}	6.58

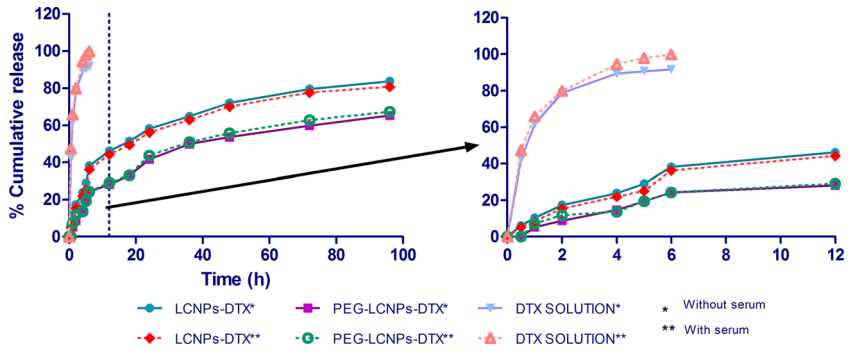

Fig. 2 *In-vitro* drug release profile of various DTX loaded LCNPs.

LCNPs-DTX (~13 h). Similar trend was also noted in case of total area under curve (AUC) suggesting the relatively higher circulation potential of PEG-LCNPs.

Antitumor Efficacy

Figure 6 reveals the percentage change in tumor volume of animal groups treated with control, Taxotere®, LCNPs-DTX and PEG-LCNPs-DTX. As evident, significant increase in the tumor volume was noted in case of control group leading to ~170% increase in tumor burden within 10 days. In contrast, consistent decrease in the tumor volume was noted in all the treatment groups. However, the reduction in tumor volume was significantly higher in case of PEG-LCNPs-DTX as compared to that of Taxotere®. Among developed LCNPs, higher reduction in case of PEG-LCNPs-DTX was noted as compared to that of LCNPs-DTX., no statistical significant difference in the antitumor efficacy of the LCNPs-DTX and Taxotere® was noted. After 10 days, the residual tumor burden was found out to be ~53, ~49 and ~19% in case of Taxotere®, LCNPs-DTX and PEG-LCNPs-DTX treated groups, respectively. Furthermore, the biodistribution studies revealed remarkably higher distribution of PEG-LCNPs within the tumor tissues as compared to that of LCNPs (Fig. 6c).

Toxicity Studies

Severe anaphylactic hypersensitivity reactions were noted in case of Taxotere® with sudden death of animals. Hence, the prophylactic and concomitant therapy of corticosteroids was employed in case of Taxotere® treated animals. Notably even upon concomitant corticosteroids therapy, severe tail necrosis was observed in case of Taxotere®. Furthermore, significant increase ($P<0.001$) in the levels of various biochemical parameters such as BUN, creatinine, ALT and AST were noted in case of Taxotere® as compared to that of control (Fig. 7). Conversely, in case of developed LCNPs formulations no such alterations in the levels were noted as compared to that of control suggestive of the safety profile of DTX-LCNPs.

Table III Correlation Coefficient for Different Release Models of Drug Release from Various DTX Loaded Formulations

Release model	LCNPs-DTX	PEG-LCNPs-DTX
Zero order	0.7634	0.8599
First order	0.9079	0.9255
Hixson-Crowell	0.9861	0.9709
Higuchi	0.9405	0.9884
KorsemeyerPeppas (slope)	0.9527 (0.5178)	0.9707 (0.4692)

DISCUSSION

Surface functionalized LCNPs were prepared by dilution through hydrotrope method (15) and optimized exhaustively to ensure robust formulation (Table S1). The employed method is quite simple and does not require any high energy inputs (8). The optimization studies revealed that stable LCNPs could be prepared using Pluronic® F 108 (0.5%*w/v*) as stabilizer owing to the least solubility of DTX (Table S2 and Table S3). These high molecular weight nonionic triblock copolymers are capable of adsorbing at the interface of LCNPs thereby exhibiting relatively greater stabilization apart from playing classical role of surfactant i.e., preventing aggregation of mesophases (26). Subsequently, hydrotrope concentration was also optimized for maximizing the entrapment efficiency (Table S4) and optimization of the theoretical drug loading (Table S5). The prepared LCNPs were then surface functionalized *via* DSPE-PEG to impart stealth properties. The optimization of surface functionalization further

Table IV *In Vitro* Cytotoxicity of Various DTX Loaded Formulations

Incubation time (h)	IC_{50} (μg/ml)		
	Free DTX	LCNPs-DTX	PEG-LCNPs-DTX
24	3.873 ± 0.63	0.283 ± 0.16	0.181 ± 0.09
48	2.529 ± 0.49	0.228 ± 0.15	0.098 ± 0.03

All values are expressed as mean ± SD ($n = 6$)

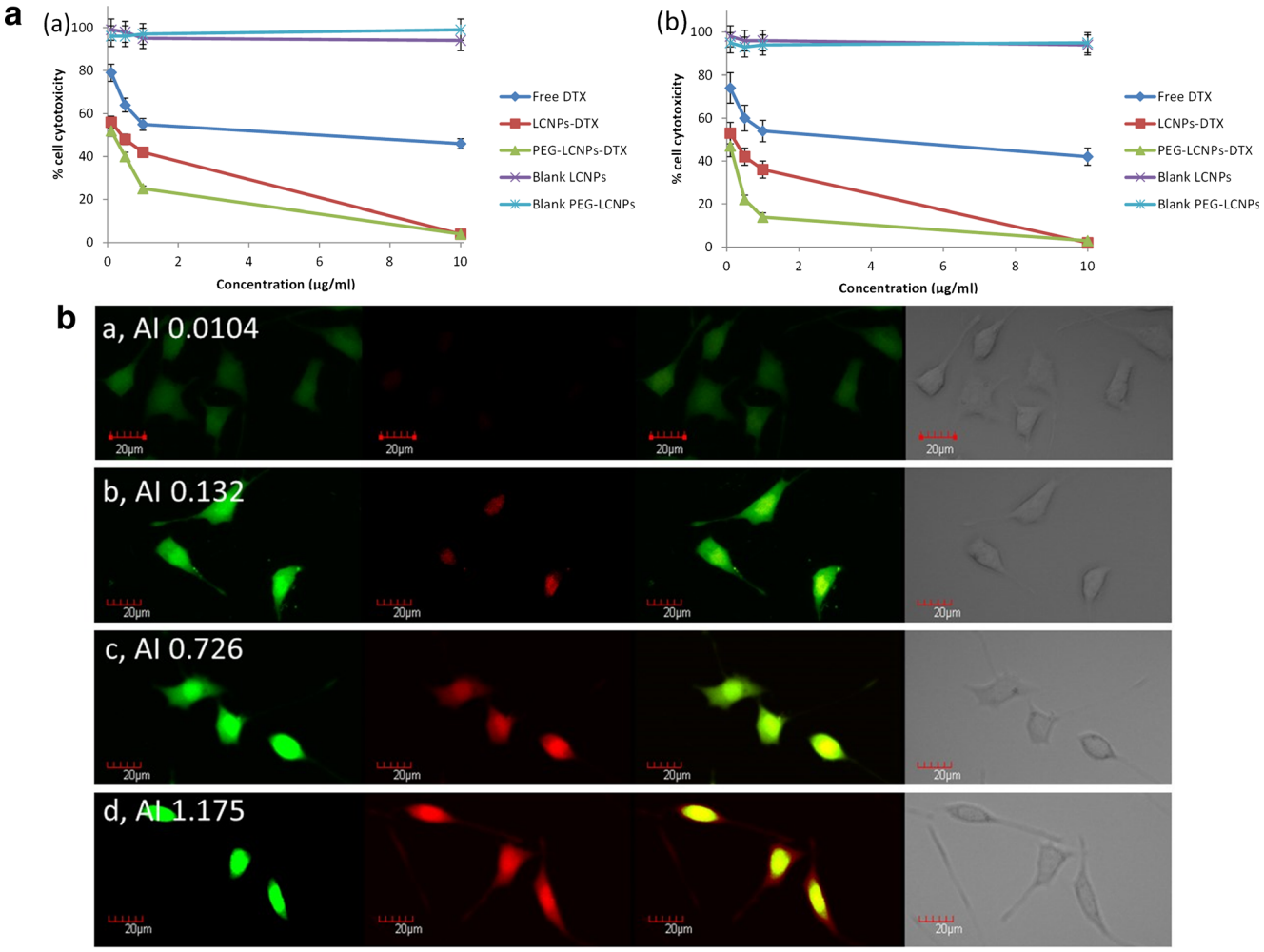

Fig. 3 (**a**) Cell cytotoxicity of DTX loaded LCNPs upon incubation for (i) 24 h and (ii) 48 h. (**b**) Representative images showing apoptosis in cells treated with (*a*) control (vehicle treated), (*b*) free DTX (*c*) LCNPs-DTX and (*d*) PEG-LCNPs-DTX equivalent to 5 μg/ml DTX for 3 h. Green channel represents the fluorescence from 6-Carboxyfluorescein while red channel depicts fluorescence from Annexin V-Cy3.18 conjugate. *AI* Apoptosis index.

revealed a decreasing trend in the zeta potential of the LCNPs with increase in concentration of mPEG-DSPE in case of PEGylated LCNPs. This could be owing to the negatively charged phosphate group thus eliciting a reduced electrophoretic mobility (Table S6). Finally, the optimized formulations were lyophilized using mannitol as cryo-protectant owing to its good cake forming capability and stabilizing effects on the original quality attributes of the LCNPs (Figure S2). Insignificant changes in the critical quality attributes such as particle size, PDI and entrapment efficiency were noted upon reconstitution. The Sf/Si ratio (ratio of particle size before and after lyophilization) was found to be <1.5 in all the cases with reconstitution time <1 min (Table S7). The final optimized quality attributes of the developed LCNPs are depicted in Table I.

The morphological evaluation of the developed formulations by TEM revealed cubic and hexagonal nanostructures in all the cases (Table II). The diversity in the structures could be attributed to the partition of DTX (hydrophobic drug) into the hydrophobic domains of the cubic phase. This leads to altered lipid bilayer contortion thereby affecting the cubic texture and the geometry of the dispersed LCNPs (27). Slight irregular geometries were noted in case of PEG-LCNPs-DTX which could be attributed to the surface functionalization of LCNPs (Fig. 1). The microscopic observations by TEM were further corroborated by SAXS analysis which revealed a slight decrease in the lattice constant of DTX-LCNPs as compared to that of blank LCNPs suggestive of DTX orientation within lipid matrices (28).

In vitro drug release studies proved the sustained release capabilities of the developed LCNPs (Fig. 2). The modelling of the release pattern revealed Hixson-Crowell kinetics as preferential mechanism for drug release from LCNPs-DTX suggestive of the surface erosion and transitions into secondary structures of the LCNPs. Upon surface functionalization, the release kinetics shifted towards Higuchi type indicative of matrix dependent drug release pattern of DTX (Table III). Furthermore, the slope of Korsemeyer Peppas model revealed

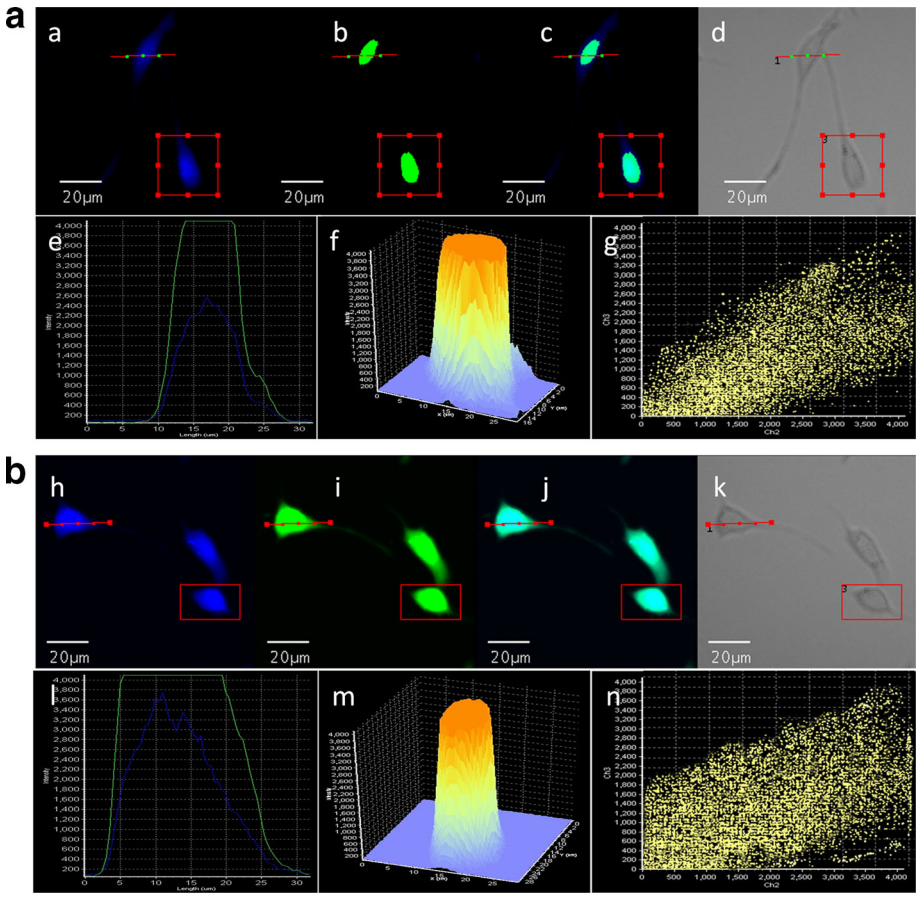

Fig. 4 Nuclear co-localization of (**a**) C-6 loaded LCNPs (**b**) C-6 loaded PEG LCNPs. *a* and *h* represent the DAPI stained nucleus of MCF-7 cells whereas *b* and *i* depict the localization of coumarin-6 loaded LCNPs and C-6 loaded PEG LCNPs in the same cells. *c* and *i* reflect the overlay images of *a* and *b* and *h* and *i*, respectively; *d* and *k* shows (DIC image) of the treated cells , respectively. The line analysis plots (*e* and *l*) and box analysis (*f* and *m*) show interaction of DAPI and coumarin-6 and NR–coumarin-6 dyes interaction, respectively. Scale bar denotes 20 μm.

anomalous diffusion through tortuous pathway for drug release from LCNPs owing to surface functionalization (20). The results were in line with our previous report (15).

The *in vitro* cell culture experiments further revealed the cytotoxic potential of developed formulations exhibiting 25.80-fold decrease in the IC_{50} value for PEG-LCNPs-DTX as compared to free DTX upon incubation with MCF-7 cells for 48 h (Fig. 3a). Such significant increase in the cell

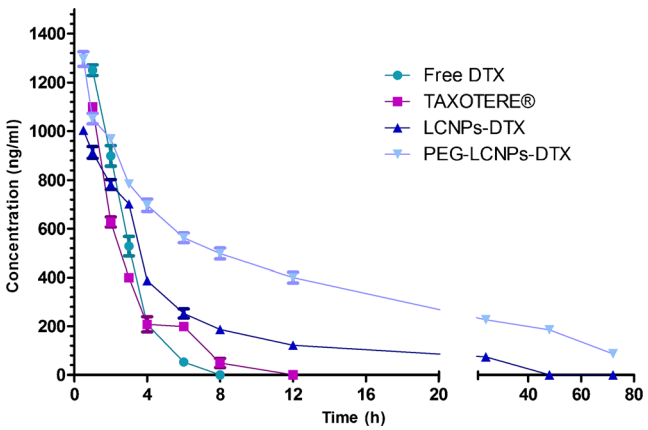

Fig. 5 Plasma Concentration time profiles of DTX loaded various LCNPs formulations upon *i.v.* administration in rats.

cytotoxicity could be attributed to relative sustained release of drug from PEGylated carriers and P-gp inhibitory activity of PEGs and Pluronics (Table IV) (9). The cell uptake of LCNPs occurs through membrane modifying properties (fluidity or fusion) owing to bioadhesiveness of phytantriol (15). However, the PEGylated carriers are preferentially uptaken by energy dependent lipid raft mediated but caveolae independent endocytosis (29). Notably, the discrepancy associated with the relatively higher uptake of PEGylated LCNPs as compared to plain LCNPs could to attributed to bioadhesive nature of phytantriol thereby limiting internalization within cells and superior bio-nano interactions of PEGylated nanocarriers as compared to the non PEGylated counterparts. Recent reports suggests that moderately PEGylated nanocarriers (1–2 kD) shows higher cellular uptake in cancer cells to non PEGylated and highly PEGylated (~5kD) nanocarriers (30). The predominant role of carrier degradation within the cell and release of free drug for imparting therapeutic response has also been recently established. Unfortunately, owing to the limitations of the analytical techniques, it is practically not feasible to assess the free drug and drug encapsulated in nanoparticles within the cells. The apoptosis assay followed by nuclear co localization studies further testified the remarkably higher toxicity of the PEG-LCNPs as

Table V Pharmacokinetic Parameters of Various DTX Loaded Nanoformulations

Parameters	Free DTX	Taxotere®	LCNPs-DTX	PEG-LCNPs-DTX
C_{30min} (ng/ml)	1708.67 ± 25.43	1575.28 ± 41.34	1003.76 ± 40.20	1296.09 ± 71.80
AUC (0–24) (ng/ml h)	4209.92 ± 24.42	4023.59 ± 23.55	6358.11 ± 24.44	16,984.56 ± 74.15
AUC (0-∞) (ng/ml h)	4282.21 ± 34.84	4137.95 ± 51.12	7683.04 ± 31.63	21,836.23 ± 316.42
$T_{1/2}$ (h)	0.95 ± 0.08	1.55 ± 0.20	12.83 ± 6.51	22.41 ± 3.60

All values are expressed as mean ± SEM ($n = 6$)

compared to LCNPs and free DTX (Fig. 4a and b). The nuclear co-localization of LCNPs could be attributed to the surfactant stabilizer, Pluronic F108, which is reported to increase the nuclear transfer by acting independently as biological response modifier (31). Further it is hypothesized that owing to higher bioadhesiveness, these systems tends to escape the endosomes and enter the cellular compartment once internalized. In addition, PEGylated nanocarrier which are absorbed by lipid raft mediated endocytosis directly enter cellular compartment bypassing lysosomal pathway (32).

The delivery potential of the developed formulations was further assessed using *in vivo* pharmacokinetic studies which revealed 14.45-fold and 23.58-fold enhancement in circulation half-life of DTX upon incorporation in to PEG-LCNPs as compared to marketed formulation Taxotere® and free drug, respectively (Fig. 5). Notably, remarkable appreciation in the circulation half-life was also noted in case of PEG-LCNPs as compared to that of plain LCNPs which is of the order of 1.75-fold (Table V). Furthermore, 5.27-fold and 5.09-fold increase in the AUC $_{(0-\infty)}$ was observed in case of PEG-LCNPs-DTX as compared to Taxotere® and free DTX, respectively, which could be attributed to the higher circulation half-life owing to increased surface hydrophilicity imparted by surface PEG chains.

The efficacy potential of the developed LCNPs was further assessed using DMBA induced breast cancer model in female rats. About ~81% reduction in the tumor burden was observed with PEG-LCNPs-DTX. However, the clinical formulation, Taxotere® could reduce the tumor volume for only up to 47% whereas LCNPs-DTX could reduce it up to 51% (Fig. 6). The significantly higher antitumor efficacy of surface functionalized nanoformulations could be attributed to its high tumor-specific accumulation (Fig. 6c). In addition. factors such as enhanced permeability and retention (EPR) effect, mediated by the short, hydrophilic, PEG-like chain adhered to the surface of LCNPs (passive targeting), rapid uptake of LCNPs and their high intracellular penetrability facilitates higher localization of drug within tumor tissues (7, 15, 29).

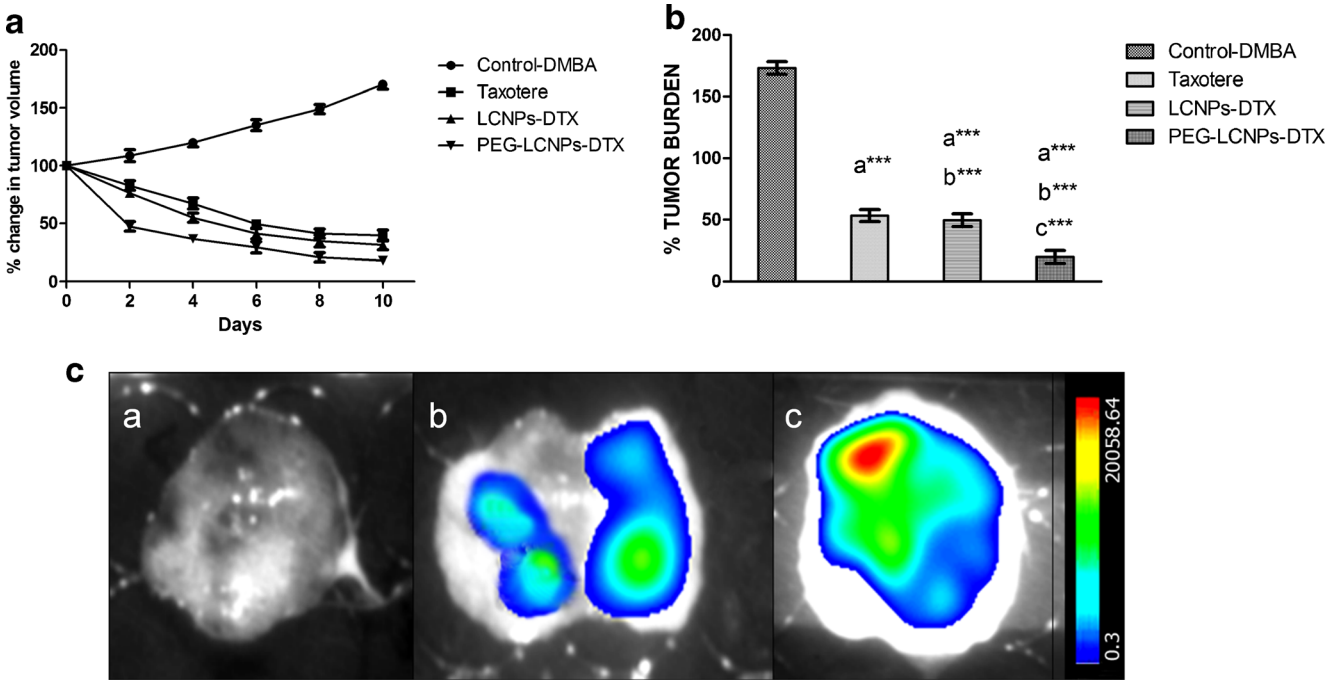

Fig. 6 (**a**) Comparison of % change in tumor volume and (**b**) % tumor burden of different formulations in tumors. (**c**) Representative images of tumor excised from animals treated with (*a*) control (vehicle treated), (*b*) coumarin-6 loaded LCNPs-DTX and (*c*) coumarin-6 loaded PEG-LCNPs-DTX formulations depicting fluorescence originated from coumarin-6. (*** = significant difference at $p < 0.001\%$, ** = significant difference at $p < 0.01\%$ and * = significant difference at $p < 0.05\%$). Tumor burden represents the ratio of residual tumor volume at a particular time to that of original tumor volume before starting of any treatment.

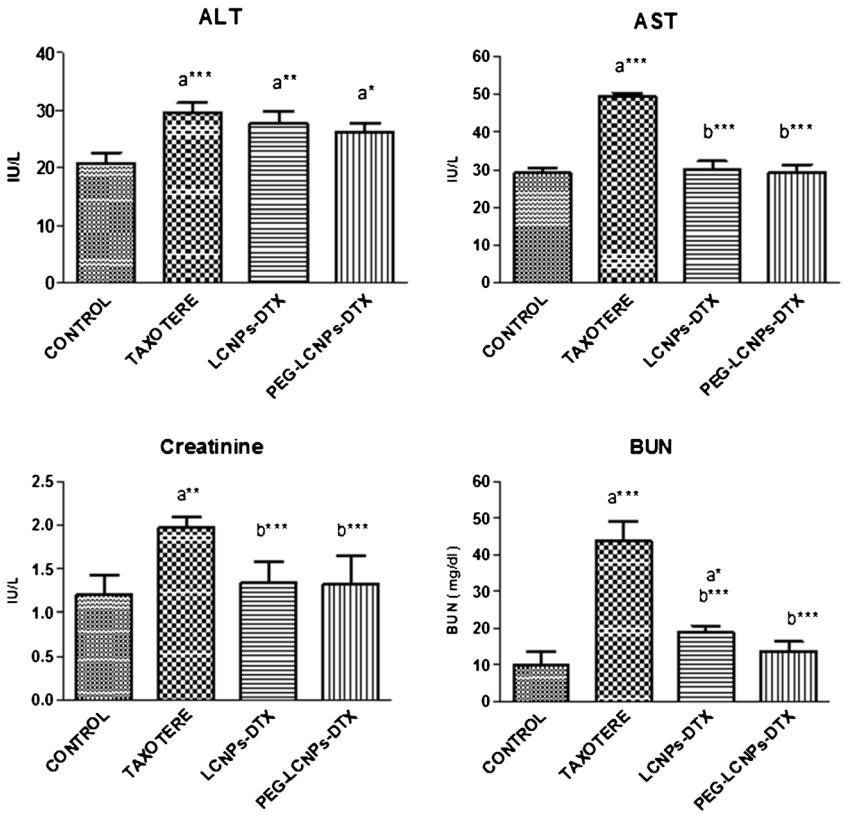

Fig. 7 Toxicity profiling of DTX loaded formulations. All values are expressed as mean ± SD ($n = 5$), *** = significant difference at $p < 0.001\%$, ** = significant difference at $p < 0.01\%$, * = significant difference at $p < 0.05$, a = compared to control).

Vehicle associated toxicity of Taxotere® is widely reported and is major concern in DTX based therapy (33, 34). Hence, it is mandatory to use corticosteroids in case of Taxotere® due to 100% mortality (instant death) upon intravenous administration. However, severe tail necrosis was still observed even with corticosteroids demonstrating very poor safety profile of clinical formulation. In contrast, no such observations were made in case of LCNPs. Further, nephrotoxicity induced by DTX has also been reported in literature (35). In addition, DTX is primarily excreted by hepatobiliary extraction. So toxicity studies were carried out. All the biochemical parameters were significantly higher in case of Taxotere® as compared to control ($P < 0.0001$) corroborating with the visual observations (Fig. 7). Conversely, insignificant differences in the levels of biochemical parameters of animals treated with LCNPs and that of control were observed revealing absence of any marked toxicity of the developed formulations. Such discrepancies in the safety profile could be attributed to the superior encapsulation of drug within the lipid matrices, sustained drug release profile and preferential localization of the LCNPs within the vicinity of tumor by virtue of EPR effect (15). *Per se*, the points these differences may not be clinically relevant. However, it gives some insights on safety potential of the developed formulations. The toxicity studies along with the antitumor efficacy and pharmacokinetics established the therapeutic potential of developed formulation in improving the deliverability of DTX as compared to the clinical formulation, Taxotere®.

CONCLUSION AND FUTURE PERSPECTIVES

Surface functionalized LCNPs were evaluated for their ability in improving the therapeutic potential of DTX. Significant improvements in the pharmacokinetic profile and therapeutic efficacy of the developed formulations was noted. Employing heterobi-functional PEG spacers further surface modification with homing targeting ligands such as hyaluronic acid, folic acid, etc. could be achieved to develop targeted drug delivery systems. The implications of other functional targeting ligand such as methotrexate could further be explored to impart the dual drug loading characteristics to the LCNPs which otherwise is a challenge. Subsequently, multiple dose kinetics can also be sought to further improve upon the therapeutic efficacy of the drugs.

ACKNOWLEDGMENTS AND DISCLOSURES

The authors are thankful to Director, NIPER for financial support, necessary infrastructure and facilities. N.K.S and K.T. are grateful to Council of Scientific and Industrial Research (CSIR), GOI, New Delhi, for providing research fellowships. The technical support rendered by Mr. Rahul Mahajan is also duly acknowledged.

REFERENCES

1. Bissery MC, Nohynek G, Sanderink GJ, Lavelle F. Docetaxel (Taxotere): a review of preclinical and clinical experience. Part I: preclinical experience. Anticancer Drugs. 1995;6(3):339–355–63–338.
2. Cervin C, Tinzl M, Johnsson M, Abrahamsson PA, Tiberg F, Dizeyi N. Properties and effects of a novel liquid crystal nanoparticle formulation of docetaxel in a prostate cancer mouse model. Eur J Pharm Sci. 2010;41(2):369–75.
3. Baker SD, Li J, ten Tije AJ, Figg WD, Graveland W, Verweij J, *et al.* Relationship of systemic exposure to unbound docetaxel and neutropenia. Clin Pharmacol Ther. 2005;77(1):43–53.
4. Engels FK, Sparreboom A, Mathot RA, Verweij J. Potential for improvement of docetaxel-based chemotherapy: a pharmacological review. Br J Cancer. 2005;93(2):173–7.
5. Guo C, Wang J, Cao F, Lee RJ, Zhai G. Lyotropic liquid crystal systems in drug delivery. Drug Discov Today. 2010;15(23–24):1032–40.
6. Rizwan SB, Boyd BJ, Rades T, Hook S. Bicontinuous cubic liquid crystals as sustained delivery systems for peptides and proteins. Expert Opin Drug Deliv. 2010;7(10):1133–44.
7. Swarnakar NK, Thanki K, Jain S. Enhanced antitumor efficacy and counterfeited cardiotoxicity of combinatorial oral therapy using Doxorubicin- and Coenzyme Q10-liquid crystalline nanoparticles in comparison with intravenous Adriamycin. Nanomedicine. 2014;10(6):1231–41.
8. Spicer PT, Hayden KL, Lynch ML, Ofori-Boateng A, Burns JL. Novel process for producing cubic liquid crystalline nanoparticles (cubosomes). Langmuir. 2001;17(19):5748–56.
9. Thanki K, Gangwal RP, Sangamwar AT, Jain S. Oral delivery of anticancer drugs: challenges and opportunities. J Control Release. 2013;170(1):15–40.
10. Drummondand CJ, Fong C. Surfactant self-assembly objects as novel drug delivery vehicles. Curr Opin Colloid Interface Sci. 1999;4(6):449–56.
11. Lawrence ASC, Bingham A, Capper CB, Hume K. The penetration of water and aqueous soap solutions into fatty substances containing one or two polar groups. J Phys Chem. 1964;68(12):3470–6.
12. Lancelot A, Sierra T, Serrano JL. Nanostructured liquid-crystalline particles for drug delivery. Expert Opin Drug Deliv. 2014;11(4):547–64.
13. Barauskas J, Cervin C, Jankunec M, Spandyreva M, Ribokaite K, Tiberg F, *et al.* Interactions of lipid-based liquid crystalline nanoparticles with model and cell membranes. Int J Pharm. 2010;391(1–2):284–91.
14. Pan X, Han K, Peng X, Yang Z, Qin L, Zhu C, *et al.* Nanostructed cubosomes as advanced drug delivery system. Curr Pharm Des. 2013;19(35):6290–7.
15. Swarnakar NK, Thanki K, Jain S. Bicontinuous cubic liquid crystalline nanoparticles for oral delivery of Doxorubicin: implications on bioavailability, therapeutic efficacy, and cardiotoxicity. Pharm Res. 2014;31(5):1219–38.
16. Yamashita F, Hashida M. Pharmacokinetic considerations for targeted drug delivery. Adv Drug Deliv Rev. 2013;65(1):139–47.
17. Kolate A, Baradia D, Patil S, Vhora I, Kore G, Misra A. PEG - a versatile conjugating ligand for drugs and drug delivery systems. J Control Release. 2014;192:67–81.
18. Maeda H, Wu J, Sawa T, Matsumura Y, Hori K. Tumor vascular permeability and the EPR effect in macromolecular therapeutics: a review. J Control Release. 2000;65(1–2):271–84.
19. Wicki A, Witzigmann D, Balasubramanian V, Huwyler J. Nanomedicine in cancer therapy: challenges, opportunities, and clinical applications. J Control Release. 2014;200(C):138–57.
20. Jain V, Swarnakar NK, Mishra PR, Verma A, Kaul A, Mishra AK, *et al.* Paclitaxel loaded PEGylated gleceryl monooleate based nanoparticulate carriers in chemotherapy. Biomaterials. 2012;33(29):7206–20.
21. Jain AK, Thanki K, Jain S. Solidified self-nanoemulsifying formulation for oral delivery of combinatorial therapeutic regimen: part II in vivo pharmacokinetics, antitumor efficacy and hepatotoxicity. Pharm Res. 2014;31(4):946–58.
22. Jain S, Jain AK, Pohekar M, Thanki K. Novel self-emulsifying formulation of quercetin for improved in vivo antioxidant potential: Implications for drug-induced cardiotoxicity and nephrotoxicity. Free Radic Biol Med. 2013;65C:117–30.
23. Swarnakar NK, Thanki K, Jain S. Effect of co-administration of CoQ10-loaded nanoparticles on the efficacy and cardiotoxicity of doxorubicin-loaded nanoparticles. RSC Adv. 2013;3(34):14671–85.
24. Choi BC, Choi JS, Han HK. Altered pharmacokinetics of paclitaxel by the concomitant use of morin in rats. Int J Pharm. 2006;323(1–2):81–5.
25. Jain AK, Swarnakar NK, Godugu C, Singh RP, Jain S. The effect of the oral administration of polymeric nanoparticles on the efficacy and toxicity of tamoxifen. Biomaterials. 2011;32(2):503–15.
26. Johnsson M, Lam Y, Barauskas J, Tiberg F. Aqueous phase behavior and dispersed nanoparticles of diglycerol monooleate/glycerol dioleate mixtures. Langmuir. 2005;21(11):5159–65.
27. Changand C-M, Bodmeier R. Binding of drugs to monoglyceride-based drug delivery systems. Int J Pharm. 1997;147(2):135–42.
28. Swarnakar NK, Thanki K, Jain S. Lyotropic liquid crystalline nanoparticles of CoQ10: implication of lipase digestibility on oral bioavailability, in vivo antioxidant activity, and in vitro-in vivo relationships. Mol Pharm. 2014;11(5):1435–49.
29. Vandana M, Sahoo SK. Long circulation and cytotoxicity of PEGylated gemcitabine and its potential for the treatment of pancreatic cancer. Biomaterials. 2010;31(35):9340–56.
30. Pozzi D, Colapicchioni V, Caracciolo G, Piovesana S, Capriotti AL, Palchetti S, *et al.* Effect of polyethyleneglycol (PEG) chain length on the bio-nano-interactions between PEGylated lipid nanoparticles and biological fluids: from nanostructure to uptake in cancer cells. Nanoscale. 2014;6(5):2782–92.
31. Yang Z, Sahay G, Sriadibhatla S, Kabanov AV. Amphiphilic block copolymers enhance cellular uptake and nuclear entry of polyplex-delivered DNA. Bioconjug Chem. 2008;19(10):1987–94.
32. Song Q, Wang X, Hu Q, Huang M, Yao L, Qi H, *et al.* Cellular internalization pathway and transcellular transport of pegylated polyester nanoparticles in Caco-2 cells. Int J Pharm. 2013;445(1–2):58–68.
33. Panday VRN, Huizing MT, Huinink WWTB, Vermorken JB, Beijnen JH. Hypersensitivity reactions to the taxanes paclitaxel and docetaxel. Clin Drug Investig. 1997;14(5):418–27.
34. Norris LB, Qureshi ZP, Bookstaver PB, Raisch DW, Sartor O, Chen H, *et al.* Polysorbate 80 hypersensitivity reactions: a renewed call to action. Commun Oncol. 2010;7(9):425–8.
35. Takimoto T, Nakabori T, Osa A, Morita S, Terada H, Oseto S, *et al.* Tubular nephrotoxicity induced by docetaxel in non-small-cell lung cancer patients. Int J Clin Oncol. 2012;17(4):395–8.